

Journal of Mechanics of Materials and Structures

**SIFS OF RECTANGULAR TENSILE SHEETS
WITH SYMMETRIC DOUBLE EDGE DEFECTS**

Xiangqiao Yan, Baoliang Liu and Zhaohui Hu

Volume 5, No. 5

May 2010



mathematical sciences publishers

SIFS OF RECTANGULAR TENSILE SHEETS WITH SYMMETRIC DOUBLE EDGE DEFECTS

XIANGQIAO YAN, BAOLIANG LIU AND ZHAOHUI HU

Tensile sheets with symmetrically placed cracks on opposite edges are studied using the displacement discontinuity method with crack-tip elements. Three cases are considered: a rectangular sheet, one with half-circle indentations on the cracked edges, and one with notch indentations. Solutions for the stress intensity factors (SIFs) of the three problems are given, revealing the effect of the geometric parameters. By comparing the three cases, one observes that the indentations have a shielding effect.

1. Introduction

In plates with holes under the action of fatigue loading, crack initiation is most likely at the hole edges due to stress concentration around the hole. Consequently, a number of papers have dealt with hole edge crack problems. Bowie [1956] gave solutions for a circular hole with a single edge crack and a pair of symmetrical edge cracks in a plate under tension. Newman [1971], using the boundary collocation method, and Murakami [1978], using the body force method, analyzed the tension problem for an elliptical hole with symmetrical edge cracks. Tweed and Rooke [1973] used the Mellin transform technique to make analyses of biaxial tensions for a branching crack emanating from a circle hole. Isida and Nakamura [1980] made an analysis of a slant crack emanating from an elliptical hole under uniaxial tension and shear at infinity by using the body force method.

Here we consider the related problem of rectangular tensile sheets with symmetric double edge defects, in the shapes illustrated in Figure 1. In [Yan 2003a] we proposed a method, based on the displacement

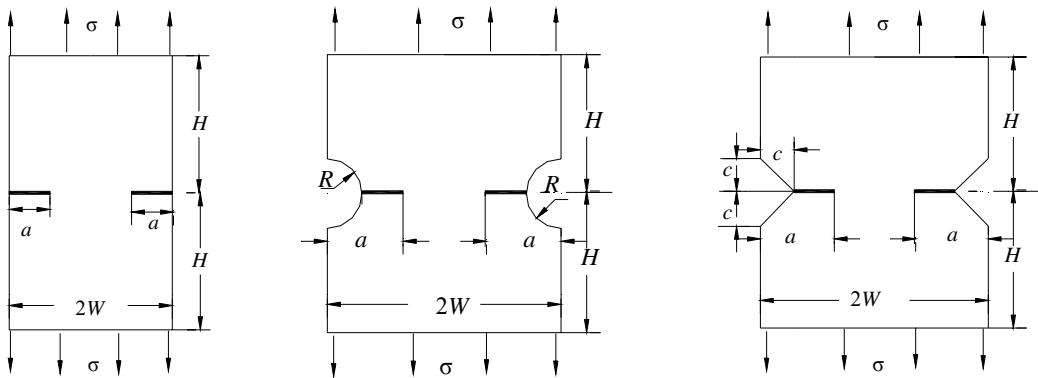


Figure 1. Rectangular tensile sheet with symmetric cracks emanating from straight edges (left), from half-circle indentations (middle), and from half-square notches (right).

Keywords: double edge defects, stress intensity factors, edge crack, half-circular indentation, half-square indentation.
Special thanks to the National Natural Science Foundation of China for supporting the present work (grant #10272037).

discontinuity method with crack-tip elements, for the analysis of general plane elastic crack problems. It was found in that paper, as well as in subsequent ones such as [Yan 2003b; 2006a; 2006b], that this method is accurate and effective for analyzing such problems.

We therefore use this method to perform a numerical analysis of the problem involving the shapes in Figure 1, focusing specifically on the stress intensity factors (SIFs). Murakami [1987] reported the SIFs for the plane elastic crack problems shown in the first two cases (simple crack and crack in semicircle indentation) when the aspect ratio H/W is large (narrow strip); but to our knowledge, detailed solutions to the SIFs for this geometry have not been obtained when H/W is less than 2. The same reference also reports the solutions to the SIFs of cracks emanating from a square hole in infinite plate in tension.

The effect of the geometric parameters of the cracked bodies on the SIFs is discussed for all three cases, and it is found that the half-circle and notch indentations have a shielding effect on the SIFs. The study illustrates the use of the boundary element method, which proves to be simply and accurate for calculating the SIFs of complex crack problems in a finite plate.

2. Brief description of the boundary element method

We briefly review the method introduced in [Yan 2003a], which in turn is based on [Crouch and Starfield 1983]. In this latter reference, the displacement discontinuity

$$D_x = u_x(x, 0_-) - u_x(x, 0_+), \quad D_y = u_y(x, 0_-) - u_y(x, 0_+), \quad (1)$$

defined as the difference in displacement between the two sides of the segment, is used to solve for the displacements, which take on the values

$$\begin{aligned} u_x &= D_x(2(1-\nu)F_3(x, y) - yF_5(x, y)) + D_y(-(1-2\nu)F_2(x, y) - yF_4(x, y)), \\ u_y &= D_x((1-2\nu)F_2(x, y) - yF_4(x, y)) + D_y(2(1-\nu)F_3(x, y) + yF_5(x, y)), \end{aligned} \quad (2)$$

and the stresses, whose values are

$$\begin{aligned} \sigma_{xx} &= 2GD_x(2F_4(x, y) + yF_6(x, y)) + 2GD_y(-F_5(x, y) + yF_7(x, y)), \\ \sigma_{yy} &= 2GD_x(-yF_6(x, y)) + 2GD_y(-F_5(x, y) - yF_7(x, y)), \\ \sigma_{xy} &= 2GD_x(-F_5(x, y) + yF_7(x, y)) + 2GD_y(-yF_6(x, y)), \end{aligned} \quad (3)$$

In these equations, G is the shear modulus and ν the Poisson's ratio; the functions F_2 through F_7 are described in [Crouch and Starfield 1983].

By using (2) and (3), we gave formulas in [Yan 2003a] for the left and right crack-tip displacement discontinuity elements. For the left crack-tip, the displacement discontinuity functions are chosen as

$$D_x = H_s \left(\frac{a_{\text{tip}} + \xi}{a_{\text{tip}}} \right)^{1/2}, \quad D_y = H_n \left(\frac{a_{\text{tip}} + \xi}{a_{\text{tip}}} \right)^{1/2}, \quad (4)$$

where H_s and H_n are the tangential and normal displacement discontinuities at the center of the element, and a_{tip} is half the length of crack-tip element. Note that the element has the same unknowns as the two-dimensional constant displacement discontinuity element. We have shown that the displacement discontinuity functions in (4) can model the displacement fields around the crack tip. The stress field determined by the displacement discontinuity functions (4) has an $r^{-1/2}$ singularity around the crack tip.

Based on (2) and (3), the displacements at a point (x, y) due to the left crack-tip displacement discontinuity element can be obtained as

$$\begin{aligned} u_x &= H_s(2(1-\nu)B_3(x, y) - yB_5(x, y)) + H_n(-(1-2\nu)B_2(x, y) - yB_4(x, y)), \\ u_y &= H_s((1-2\nu)B_2(x, y) - yB_4(x, y)) + H_n(2(1-\nu)B_3(x, y) + yB_5(x, y)), \end{aligned} \quad (5)$$

and the stresses as

$$\begin{aligned} \sigma_{xx} &= 2GH_s(2B_4(x, y) + yB_6(x, y)) + 2GH_n(-B_5(x, y) + yB_7(x, y)), \\ \sigma_{yy} &= 2GH_s(-yB_6(x, y)) + 2GH_n(-B_5(x, y) - yB_7(x, y)), \\ \sigma_{xy} &= 2GH_s(-B_5(x, y) + yB_7(x, y)) + 2GH_n(-yB_6(x, y)), \end{aligned} \quad (6)$$

where the functions B_2 through B_7 are described in [Yan 2003a].

Implementation of the numerical approach. The objective of many analyses of linear elastic crack problems is to obtain the stress intensity factors K_I and K_{II} . Crouch and Starfield [1983] used relations (2) and (3) to set up the constant displacement discontinuity boundary element method. Similarly, we can use (5) and (6) to set up boundary element equations associated with the crack-tip elements. The constant displacement discontinuity element together with the crack-tip elements is combined to form a very effective numerical approach for calculating the SIFs of general plane cracks. In the boundary element implementation, the left or the right crack-tip element is placed locally at the corresponding left or right crack tip on top of the constant displacement discontinuity elements that cover the entire crack surface and the other boundaries. This is called the displacement discontinuity method with crack-tip elements. Based on the displacement field around the crack tip, we can write

$$K_I = -\frac{\sqrt{2\pi}GH_n}{4(1-\nu)\sqrt{a_{\text{tip}}}}, \quad K_{II} = -\frac{\sqrt{2\pi}GH_s}{4(1-\nu)\sqrt{a_{\text{tip}}}}, \quad (7)$$

3. Numerical results and discussion

We report here the results of SIF calculations for the plane elastic crack problems of Figure 1. We start with the simple rectangular plate (left in the figure), taking the following ratios:

$$a/W = 0.1, 0.2, 0.3, 0.4, 0.5, 0.6, 0.7$$

$$H/W = 0.4, 0.5, 0.6, 0.7, 0.8, 0.9, 1.0, 1.2, 1.5, 2.0$$

Regarding discretization, 30 boundary elements with of equal size, $a/30$, on the right edge crack are discretized and the other boundaries are discretized according to the limitation that all boundary elements have approximately the same length [Yan 2003a]. The calculated SIFs normalized by $\sigma\sqrt{\pi a}$ are given in Table 1. For comparison, the table also lists the numerical results reported in [Murakami 1987], with which our numerical results are in good agreement.

Table 1 makes it clear that one must consider the effect of H/W on the SIF:

- (1) For a shallow defect ($a/W = 0.1$) the SIF with a $H/W = 0.4$ (low aspect ratio) is 16% larger than that when $H/W = 2$.

a/W	H/W										liter.
	0.4	0.5	0.6	0.7	0.8	0.9	1.0	1.2	1.5	2.0	
0.1	1.2902	1.2344	1.2007	1.1773	1.1596	1.1459	1.1356	1.1228	1.1154	1.1129	–
0.2	1.6499	1.4900	1.3879	1.3139	1.2576	1.2142	1.1820	1.1425	1.1193	1.1123	1.118
0.3	2.0845	1.8093	1.6213	1.4813	1.3750	1.2959	1.2386	1.1700	1.1305	1.1183	1.120
0.4	2.5464	2.1422	1.8537	1.6393	1.4834	1.3719	1.2943	1.2045	1.1536	1.1377	1.132
0.5	2.9943	2.4333	2.0329	1.7521	1.5611	1.4315	1.3449	1.2478	1.1937	1.1765	1.163
0.6	3.3400	2.5980	2.1104	1.8006	1.6046	1.4792	1.3979	1.3090	1.2603	1.2446	1.226
0.7	3.3959	2.5553	2.0776	1.8032	1.6406	1.5410	1.4782	1.4107	1.3739	1.3618	1.343

Table 1. Normalized SIFs for the rectangular plate in Figure 1, left. Literature values on the last column, taken from [Murakami 1987], refer to a high value of H/W .

(2) As a/W increases, this effect becomes more obvious. For $a/W = 0.6$, for example, the SIF when $H/W = 0.4$ is 2.68 times the one when $H/W = 2.0$. But when H/W is larger than 2 this effect is negligible regardless of the size of a/W , which perhaps is the reason for taking $H/W = 2$ in calculating the SIFs of crack problems in finite width plates [Newman 1971].

Cracks emanating from half-circle indentations. Two sorts of experiments are reported for the geometry shown in Figure 1, middle. First, we consider a crack that is much larger than the corresponding indentation, to approximate the situation just discussed, where the crack emanates from a straight edge. For example, if we take

$$H/W = 1, \quad a/R = 7, \quad a/W = 0.5,$$

we expect that the effect of the half-circle indentation on the SIFs will be negligible. For the discretization, the number of boundary elements on a quarter-circle is taken as 50 and the other boundaries are discretized according to the limitation that all boundary elements have approximately the same length. The calculated SIF normalized by $\sigma\sqrt{\pi a}$ is 1.3200, which is indeed close to the corresponding value (1.3449) listed in Table 1.

Secondly, we systematically vary the three relevant ratios to study their effect on the SIF. The following cases are considered:

$$\begin{aligned} a/R &= 1.02, 1.04, 1.06, 1.08, 1.1, 1.15, 1.2, 1.5, 2.0 \\ H/W &= 0.5, 0.6, 0.7, 0.8, 0.9, 1.0, 1.5, 2.0 \\ a/W &= 0.2, 0.3, 0.4, 0.5, 0.6, 0.7 \end{aligned}$$

For the discretization, the number of boundary elements on a quarter-circle is chosen according to a/R as follows:

a/R	1.02	1.04	1.06	1.08	1.1	1.15	1.2	1.5	2.0
# elements	250	200	167	175	160	133	100	100	50

The other boundaries are discretized so that all boundary elements have approximately the same length. The calculated SIFs normalized by $\sigma\sqrt{\pi a}$ are given in Table 2.

To study the effect of the half-circle indentations on the SIF, we compare the numbers in Table 2 with those in Table 1. Recall that Table 1 corresponds to a ratio $a/R = \infty$. We find that, as a/R increases

H/W	a/R									
	1.02	1.04	1.06	1.08	1.1	1.15	1.2	1.5	2.0	
$a/W = 0.2$	0.5	0.5949	0.8122	0.9541	1.0511	1.1284	1.2528	1.3298	1.4469	1.4701
	0.6	0.5526	0.7558	0.8883	0.9796	1.0523	1.1700	1.2413	1.3525	1.3719
	0.7	0.5211	0.7141	0.8402	0.9270	0.9969	1.1093	1.1774	1.2835	1.3008
	0.8	0.4969	0.6822	0.8029	0.8866	0.9532	1.0620	1.1282	1.2304	1.2469
	0.9	0.4782	0.6575	0.7743	0.8555	0.9204	1.0263	1.0905	1.1899	1.2053
	1.0	0.4645	0.6394	0.7533	0.8327	0.8959	0.9994	1.0625	1.1599	1.1745
$a/W = 0.3$	0.5	0.7321	0.9937	1.1663	1.2812	1.3765	1.5247	1.6161	1.7600	1.7909
	0.6	0.6507	0.8856	1.0396	1.1452	1.2298	1.3648	1.4478	1.5776	1.6036
	0.7	0.5903	0.8048	0.9449	1.0430	1.1202	1.2453	1.3231	1.4440	1.4669
	0.8	0.5446	0.7441	0.8747	0.9664	1.0393	1.1566	1.2291	1.3437	1.3628
	0.9	0.5113	0.7000	0.8233	0.9107	0.9793	1.0915	1.1598	1.2689	1.2859
	1.0	0.4879	0.6688	0.7870	0.8707	0.9366	1.0447	1.1102	1.2150	1.2303
	1.5	0.4460	0.6128	0.7214	0.7987	0.8593	0.9589	1.0192	1.1146	1.1264
2.0	0.4410	0.6063	0.7139	0.7903	0.8505	0.9491	1.0088	1.1028	1.1147	
$a/W = 0.4$	0.5	0.8732	1.1806	1.3870	1.5282	1.6393	1.8193	1.9272	2.0990	2.1327
	0.6	0.7429	1.0081	1.1843	1.3076	1.4034	1.5606	1.6565	1.8100	1.8400
	0.7	0.6459	0.8792	1.0362	1.1444	1.2318	1.3731	1.4594	1.5988	1.6266
	0.8	0.5782	0.7898	0.9309	1.0307	1.1089	1.2385	1.3178	1.4467	1.4704
	0.9	0.5334	0.7293	0.8591	0.9525	1.0249	1.1454	1.2195	1.3405	1.3614
	1.0	0.5038	0.6896	0.8125	0.9006	0.9692	1.0834	1.1531	1.2672	1.2852
	1.5	0.4567	0.6254	0.7358	0.8151	0.8762	0.9779	1.0388	1.1373	1.1491
	2.0	0.4518	0.6189	0.7280	0.8060	0.8664	0.9665	1.0267	1.1224	1.1338
$a/W = 0.5$	0.5	0.9212	1.2521	1.4940	1.6714	1.8128	2.0510	2.1822	2.4130	2.4433
	0.6	0.7921	1.0827	1.2809	1.4204	1.5301	1.7130	1.8200	1.9978	2.0276
	0.7	0.6683	0.9162	1.0847	1.2040	1.2989	1.4577	1.5532	1.7128	1.7420
	0.8	0.5889	0.8088	0.9573	1.0637	1.1479	1.2893	1.3763	1.5232	1.5500
	0.9	0.5413	0.7428	0.8787	0.9759	1.0531	1.1827	1.2618	1.3967	1.4212
	1.0	0.5123	0.7029	0.8301	0.9218	0.9933	1.1144	1.1879	1.3134	1.3351
	1.5	0.4748	0.6489	0.7625	0.8441	0.9066	1.0110	1.0731	1.1755	1.1887
	2.0	0.4721	0.6449	0.7573	0.8374	0.8990	1.0013	1.0619	1.1603	1.1723
$a/W = 0.6$	0.6	0.7403	1.0268	1.2295	1.3895	1.5211	1.7382	1.8682	2.0894	2.1171
	0.7	0.6480	0.8978	1.0726	1.2013	1.3038	1.4778	1.5852	1.7667	1.7958
	0.8	0.5810	0.8028	0.9553	1.0669	1.1560	1.3078	1.4028	1.5664	1.5955
	0.9	0.5455	0.7505	0.8889	0.9905	1.0703	1.2066	1.2921	1.4419	1.4694
	1.0	0.5273	0.7226	0.8535	0.9476	1.0225	1.1478	1.2262	1.3632	1.3887
	1.5	0.5124	0.6964	0.8150	0.8993	0.9638	1.0695	1.1335	1.2391	1.2549
	2.0	0.5132	0.6965	0.8143	0.8974	0.9606	1.0642	1.1260	1.2261	1.2401
$a/W = 0.7$	0.7	0.6090	0.8397	1.0073	1.1430	1.2497	1.4436	1.5626	1.7776	1.8041
	0.8	0.5915	0.8125	0.9648	1.0772	1.1676	1.3259	1.4251	1.6063	1.6353
	0.9	0.5851	0.7958	0.9366	1.0383	1.1182	1.2570	1.3442	1.5041	1.5331
	1.0	0.5849	0.7905	0.9246	1.0198	1.0938	1.2200	1.2984	1.4429	1.4701
	1.5	0.5961	0.7983	0.9248	1.0115	1.0768	1.1824	1.2450	1.3507	1.3686
	2.0	0.5990	0.8022	0.9283	1.0147	1.0791	1.1821	1.2428	1.3413	1.3568

Table 2. Normalized SIFs for rectangular plate with semicircle cutout (Figure 1, middle).

from 1.02 to 2, the SIF increases monotonously regardless of the value of a/W . When a/R reaches 2, the SIF almost equals its asymptotic value in Table 1. This suggests the following observations:

- (1) The half-circle indentations have a shielding effect on the edge cracks.
- (2) The closer the depth of the indentations is to the overall defect size (that is, the lower a/R is), the larger the shielding effect.
- (3) When a/R is more than 2, meaning that the crack itself is longer than the characteristic size of the indentation, the shielding effect can be neglected.

Cracks emanating from half-square notches. We next turn to the geometry in Figure 1, right, varying the three relevant ratios to study their effect on the SIF. The following cases are considered:

$$\begin{aligned}
 a/c &= 1.02, 1.04, 1.06, 1.08, 1.1, 1.15, 1.2, 1.5, 2.0 \\
 H/W &= 0.5, 0.6, 0.7, 0.8, 0.9, 1.0, 1.5, 2.0 \\
 a/W &= 0.2, 0.3, 0.4, 0.5, 0.6, 0.7
 \end{aligned}$$

For the discretization, the number of boundary elements on a side of the notch is chosen according to a/c as follows:

a/c	1.02	1.04	1.06	1.08	1.1	1.15	1.2	1.5	2.0
# elements	250	200	167	175	160	133	100	100	50

The other boundaries are discretized so that all boundary elements have approximately the same length. The calculated SIFs normalized by $\sigma\sqrt{\pi a}$ are given in Table 3.

As in the previous subsection, we compare these numbers with those on Table 1, and see that as a/c increases from 1.02 to 2, the SIF increases monotonously regardless of the value of a/W . When a/c reaches 2, the SIF almost equals its asymptotic value in Table 1. To summarize:

- (1) The half-square notches have a shielding effect on the edge cracks.
- (2) The closer the notch depth is to the overall defect size (that is, the lower a/c is), the larger the shielding effect.
- (3) When a/c is more than 2, meaning that the crack itself is longer than the characteristic size of the notch, the shielding effect can be neglected.

Comparison between effects of half-circle and half-square indentations. We briefly compare the results for the two indented geometries: half-circle indentations versus half-square notches. Figure 2 shows the evolution of the SIF with the size of the indentation relative to the crack size, for both geometries, in two particular cases: when case $a/W = 0.2$ and $H/W = 0.5$, and when $a/W = 0.5$ and $H/W = 1.0$. We see that the shielding effect of the half-circle indentations is much stronger effect than for the notches, in agreement with the expectation that a geometry with a sharp concave angle is more vulnerable to the stress concentration effect.

H/W	a/R									
	1.02	1.04	1.06	1.08	1.1	1.15	1.2	1.5	2.0	
$a/W = 0.2$	0.5	1.3537	1.3919	1.4164	1.4240	1.4356	1.4479	1.4582	1.4595	1.4667
	0.6	1.2663	1.3018	1.3240	1.3313	1.3417	1.3530	1.3614	1.3631	1.3683
	0.7	1.2023	1.2360	1.2570	1.2636	1.2742	1.2844	1.2918	1.2928	1.2975
	0.8	1.1533	1.1858	1.2054	1.2119	1.2209	1.2312	1.2386	1.2389	1.2435
	0.9	1.1156	1.1471	1.1659	1.1721	1.1811	1.1910	1.1977	1.1979	1.2021
	1.0	1.0878	1.1184	1.1368	1.1429	1.1512	1.1607	1.1674	1.1675	1.1713
$a/W = 0.3$	0.5	1.6376	1.6881	1.7173	1.7270	1.7428	1.7583	1.7707	1.7759	1.7842
	0.6	1.4729	1.5157	1.5407	1.5503	1.5634	1.5777	1.5879	1.5924	1.5987
	0.7	1.3503	1.3905	1.4125	1.4216	1.4326	1.4442	1.4542	1.4571	1.4630
	0.8	1.2577	1.2942	1.3146	1.3227	1.3335	1.3439	1.3521	1.3552	1.3594
	0.9	1.1892	1.2237	1.2426	1.2507	1.2598	1.2698	1.2768	1.2792	1.2826
	1.0	1.1399	1.1725	1.1905	1.1980	1.2065	1.2161	1.2223	1.2243	1.2274
	1.5	1.0478	1.0773	1.0934	1.1000	1.1075	1.1155	1.1209	1.1218	1.1236
	2.0	1.0364	1.0656	1.0818	1.0880	1.0958	1.1037	1.1090	1.1096	1.1117
$a/W = 0.4$	0.5	1.9434	2.0042	2.0405	2.0545	2.0723	2.0924	2.1037	2.1141	2.1182
	0.6	1.6795	1.7304	1.7633	1.7720	1.7900	1.8074	1.8180	1.8266	1.8320
	0.7	1.4872	1.5329	1.5595	1.5700	1.5829	1.5980	1.6088	1.6149	1.6216
	0.8	1.3501	1.3898	1.4125	1.4224	1.4332	1.4473	1.4563	1.4619	1.4667
	0.9	1.2533	1.2905	1.3107	1.3202	1.3298	1.3418	1.3500	1.3544	1.3587
	1.0	1.1868	1.2212	1.2402	1.2487	1.2577	1.2689	1.2757	1.2795	1.2828
	1.5	1.0700	1.0999	1.1158	1.1231	1.1299	1.1386	1.1436	1.1453	1.1466
	2.0	1.0561	1.0856	1.1014	1.1081	1.1152	1.1237	1.1287	1.1296	1.1312
	$a/W = 0.5$	0.5	2.2054	2.2793	2.3213	2.3445	2.3649	2.3896	2.3990	2.4169
0.6		1.8419	1.9018	1.9372	1.9535	1.9698	1.9895	2.0001	2.0111	2.0128
0.7		1.5843	1.6354	1.6656	1.6776	1.6933	1.7106	1.7211	1.7305	1.7344
0.8		1.4123	1.4567	1.4827	1.4938	1.5068	1.5226	1.5329	1.5406	1.5459
0.9		1.2998	1.3394	1.3619	1.3728	1.3836	1.3976	1.4068	1.4139	1.4183
1.0		1.2265	1.2628	1.2830	1.2931	1.3024	1.3149	1.3232	1.3292	1.3331
1.5		1.1061	1.1368	1.1532	1.1611	1.1682	1.1772	1.1825	1.1850	1.1864
2.0		1.0925	1.1227	1.1387	1.1460	1.1530	1.1618	1.1668	1.1683	1.1698
$a/W = 0.6$		0.6	1.8981	1.9675	2.0061	2.0293	2.0482	2.0720	2.0819	2.0961
	0.7	1.6192	1.6749	1.7088	1.7256	1.7413	1.7612	1.7715	1.7827	1.7838
	0.8	1.4430	1.4910	1.5201	1.5334	1.5477	1.5655	1.5761	1.5866	1.5897
	0.9	1.3339	1.3770	1.4028	1.4141	1.4271	1.4431	1.4526	1.4623	1.4664
	1.0	1.2674	1.3068	1.3293	1.3402	1.3510	1.3651	1.3744	1.3825	1.3866
	1.5	1.1659	1.1983	1.2155	1.2239	1.2317	1.2416	1.2473	1.2509	1.2529
	2.0	1.1553	1.1867	1.2039	1.2116	1.2189	1.2281	1.2338	1.2358	1.2375
$a/W = 0.7$	0.7	1.6035	1.6654	1.7015	1.7240	1.7415	1.7652	1.7765	1.7901	1.7886
	0.8	1.4669	1.5193	1.5506	1.5668	1.5825	1.6026	1.6135	1.6262	1.6277
	0.9	1.3856	1.4320	1.4589	1.4734	1.4863	1.5041	1.5146	1.5265	1.5295
	1.0	1.3371	1.3804	1.4045	1.4168	1.4285	1.4444	1.4539	1.4646	1.4679
	1.5	1.2720	1.3065	1.3247	1.3339	1.3422	1.3525	1.3598	1.3641	1.3667
	2.0	1.2654	1.2990	1.3168	1.3253	1.3332	1.3431	1.3493	1.3524	1.3548

Table 3. Normalized SIFs for Double Edge Half-Square-Hole Cracks ($a/W = 0.7$)

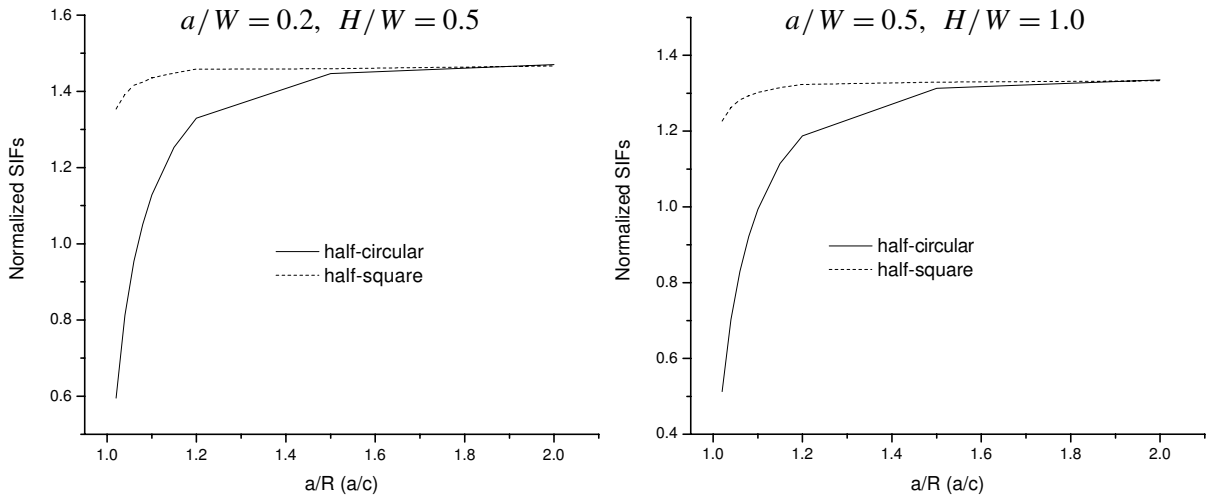


Figure 2. Effect of half-circle and half-square indentations on the SIF, for representative choices of the parameters a/W and H/W .

4. Conclusions

A numerical analysis of double edge defects in rectangular plates in tension (Figure 1) was performed, and the stress intensity factors calculated for a variety of values of the geometric parameters. By comparing the calculated SIFs for the three geometries, it was found that the presence of an indentation at the base of the crack has a shielding effect, lowering the SIF. The effect is more pronounced when the indentation is a half-circle than when it is a half-square notch. The shielding effect gradually decreases with the size of the indentation; When the characteristic size (depth) of the indentation is less than the length of the crack proper (that is, the ratio a/R or a/c in Figure 1 exceeds 2), the effect becomes negligible.

This study illustrates how the displacement discontinuity method with crack-tip elements can be of value in calculating SIFs for complex crack problems involving a finite plate.

References

- [Bowie 1956] O. L. Bowie, "Analysis of an infinite plate containing radial cracks originating at the boundary of an internal circular hole", *J. Math. Phys. (MIT)* **35** (1956), 60–71.
- [Crouch and Starfield 1983] S. L. Crouch and A. M. Starfield, *Boundary element methods in solid mechanics: with applications in rock mechanics and geological engineering*, Allen & Unwin, London, 1983.
- [Isida and Nakamura 1980] M. Isida and Y. Nakamura, "Edge cracks originating from an elliptical hole in a wide plate subjected to tension and in-plane shear", *Trans. Jpn. Soc. Mech. Eng. A* **46**:409 (1980), 947–956. In Japanese.
- [Murakami 1978] Y. Murakami, "A method of stress intensity factor calculation for the crack emanating from an arbitrarily shaped hole or the crack in the vicinity of an arbitrarily shaped hole", *Trans. Jpn. Soc. Mech. Eng.* **44**:378 (1978), 423–432. In Japanese.
- [Murakami 1987] Y. Murakami (editor), *Stress intensity factors handbook*, Pergamon, Oxford, 1987.
- [Newman 1971] J. C. Newman, Jr., "An improved method of collocation for the stress analysis of cracked plates with various shaped boundaries", NASA Technical Note TN D-6376, Langley Research Center, Hampton, VA, 1971, available at <http://hdl.handle.net/2060/19710022830>.

- [Tweed and Rooke 1973] J. Tweed and D. P. Rooke, “The distribution of stress near the tip of a radial crack at the edge of a circular hole”, *Int. J. Eng. Sci.* **11**:11 (1973), 1185–1195.
- [Yan 2003a] X. Yan, “Analysis of the interference effect of arbitrary multiple parabolic cracks in plane elasticity by using a new boundary element method”, *Comput. Methods Appl. Mech. Eng.* **192**:47–48 (2003), 5099–5121.
- [Yan 2003b] X. Yan, “An effective method of stress intensity factor calculation for cracks emanating from a triangular or square hole under biaxial loads”, *Fatigue Fract. Eng. Mater. Struct.* **26**:12 (2003), 1127–1133.
- [Yan 2006a] X. Yan, “Cracks emanating from circular hole or square hole in rectangular plate in tension”, *Eng. Fract. Mech.* **73**:12 (2006), 1743–1754.
- [Yan 2006b] X. Yan, “A numerical analysis of cracks emanating from an elliptical hole in a 2-D elasticity plate”, *Eur. J. Mech. A Solids* **25**:1 (2006), 142–153.

Received 6 Dec 2009. Revised 31 May 2010. Accepted 10 Jun 2010.

XIANGQIAO YAN: yanxiangqiao@hotmail.com

Research Laboratory on Composite Materials, Harbin Institute of Technology, Harbin 150001, China

BAOLIANG LIU: baoliangliu2008@163.com

Research Laboratory on Composite Materials, Harbin Institute of Technology, Harbin 150001, China

ZHAOHUI HU: zhaohuihu@163.com

Research Laboratory on Composite Materials, Harbin Institute of Technology, Harbin 150001, China

JOURNAL OF MECHANICS OF MATERIALS AND STRUCTURES

<http://www.jomms.org>

Founded by Charles R. Steele and Marie-Louise Steele

EDITORS

CHARLES R. STEELE Stanford University, U.S.A.
DAVIDE BIGONI University of Trento, Italy
IWONA JASIUK University of Illinois at Urbana-Champaign, U.S.A.
YASUhide SHINDO Tohoku University, Japan

EDITORIAL BOARD

H. D. BUI École Polytechnique, France
J. P. CARTER University of Sydney, Australia
R. M. CHRISTENSEN Stanford University, U.S.A.
G. M. L. GLADWELL University of Waterloo, Canada
D. H. HODGES Georgia Institute of Technology, U.S.A.
J. HUTCHINSON Harvard University, U.S.A.
C. HWU National Cheng Kung University, R.O. China
B. L. KARIHALOO University of Wales, U.K.
Y. Y. KIM Seoul National University, Republic of Korea
Z. MROZ Academy of Science, Poland
D. PAMPLONA Universidade Católica do Rio de Janeiro, Brazil
M. B. RUBIN Technion, Haifa, Israel
A. N. SHUPIKOV Ukrainian Academy of Sciences, Ukraine
T. TARNAI University Budapest, Hungary
F. Y. M. WAN University of California, Irvine, U.S.A.
P. WRIGGERS Universität Hannover, Germany
W. YANG Tsinghua University, P.R. China
F. ZIEGLER Technische Universität Wien, Austria

PRODUCTION

PAULO NEY DE SOUZA Production Manager
SHEILA NEWBERY Senior Production Editor
SILVIO LEVY Scientific Editor

Cover design: Alex Scorpan

Cover photo: Wikimedia Commons

See inside back cover or <http://www.jomms.org> for submission guidelines.

JoMMS (ISSN 1559-3959) is published in 10 issues a year. The subscription price for 2010 is US \$500/year for the electronic version, and \$660/year (+\$60 shipping outside the US) for print and electronic. Subscriptions, requests for back issues, and changes of address should be sent to Mathematical Sciences Publishers, Department of Mathematics, University of California, Berkeley, CA 94720-3840.

JoMMS peer-review and production is managed by EditFLOW™ from Mathematical Sciences Publishers.

PUBLISHED BY

 **mathematical sciences publishers**
<http://www.mathscipub.org>

A NON-PROFIT CORPORATION

Typeset in L^AT_EX

©Copyright 2010. Journal of Mechanics of Materials and Structures. All rights reserved.

- Axial compression of hollow elastic spheres** ROBERT SHORTER, JOHN D. SMITH,
VINCENT A. COVENEY and JAMES J. C. BUSFIELD 693
- Coupling of peridynamic theory and the finite element method**
BAHATTIN KILIC and ERDOGAN MADENCI 707
- Genetic programming and orthogonal least squares: a hybrid approach to
modeling the compressive strength of CFRP-confined concrete cylinders**
AMIR HOSSEIN GANDOMI, AMIR HOSSEIN ALAVI, PARVIN ARJMANDI,
ALIREZA AGHAEIFAR and REZA SEYEDNOUR 735
- Application of the Kirchhoff hypothesis to bending thin plates with different
moduli in tension and compression** XIAO-TING HE, QIANG CHEN, JUN-YI
SUN, ZHOU-LIAN ZHENG and SHAN-LIN CHEN 755
- A new modeling approach for planar beams: finite-element solutions based on
mixed variational derivations**
FERDINANDO AURICCHIO, GIUSEPPE BALDUZZI and CARLO LOVADINA 771
- SIFs of rectangular tensile sheets with symmetric double edge defects**
XIANGQIAO YAN, BAOLIANG LIU and ZHAOHUI HU 795
- A nonlinear model of thermoelastic beams with voids, with applications**
YING LI and CHANG-JUN CHENG 805
- Dynamic stiffness vibration analysis of thick spherical shell segments with variable
thickness** ELIA EFRAIM and MOSHE EISENBERGER 821
- Application of a matrix operator method to the thermoviscoelastic analysis of
composite structures** ANDREY V. PYATIGORETS, MIHAI O.
MARASTEANU, LEV KHAZANOVICH and HENRYK K. STOLARSKI 837